Silver Nanoparticles as Pigments for Water-Based Ink-Jet Inks

Shlomo Magdassi,* Amal Bassa, Yelena Vinetsky, and Alexander Kamyshny

Casali Institute of Applied Chemistry, The Hebrew University, Jerusalem, 91904, Israel

Received December 18, 2002. Revised Manuscript Received March 17, 2003

Stabilized concentrated citrate-reduced silver nanocolloids for use as pigments in ink-jet inks were prepared. Carboxymethyl cellulose was used as a polymeric stabilizer providing both electrostatic and steric stabilization. X-ray diffraction pattern, optical properties (UV−visible spectroscopy), size (TEM and dynamic light scattering), and zeta potentials of the nanoparticles were studied. It was shown that the product is silver with cubic symmetry. Absorption spectra are characterized, as a rule, by asymmetric absorption bands with maxima at 417−440 nm and shoulders at 350−352 and 380−382 nm. TEM images of unstabilized and stabilized colloids indicate the formation of nanoparticles of different shapes (spheres, hexagons, cubes, and rods) with rather wide size distribution in the range from several nanometers (spheres) up to several hundreds of nanometers (rods). CMC was found to be an effective stabilizer of silver nanoparticles, and the average particle size at CMC concentrations from 0.025 to 0.2 wt % does not exceed 50 nm. Both unstabilized and stabilized silver nanoparticles display negative zeta potentials in the pH range from 2 to 9; the maximal negative values are observed at pH 6−8 (−27 ± 5 mV for unstabilized and −33 ± 5 mV for CMC-stabilized colloids, respectively). Concentrated dispersions of silver nanoparticles (1.1 wt % of silver), which were stable for at least 7 months, were prepared by exhausted lyophilization of the freshly prepared colloids followed by redispersion. These nanoparticles in the presence of proper wetting agent, such as Disperbyk, can be used as pigments in ink-jet ink formulations for printing on various substrates (paper, glass, and transparencies). The stabilizing agent, carboxymethyl cellulose, also acts as a binder, providing good adhesion of ink to the substrates.

Introduction

Nowadays, metallic nanoparticles draw intense scientific and practical interest due to their unique properties, which differ from those of bulk and atomic species.[1−4] Such a difference is determined by peculiarity of electronic structure of the metal nanoparticles and extremely large surface area with high percentage of surface atoms. Metal nanoparticles exhibit a drastic decrease in melting point (over 500 °C for 5-nm particles of gold compared to the melting point of the bulk material[5]); they are characterized by enhanced reactivity of the surface atoms,[1,2] high electric conductivity, and unique optical properties.[6−9] Virtually, nanosized materials are well-known materials with novel properties and promising applications in electrochemistry, microelectronics, and optical, electronic, and magnetic devices and sensors[10−18] and in new types of active and selective catalysts.[1,2] Formation of stable, concentrated aqueous dispersions of metallic nanoparticles with low resistivity may offer new prospects in computer-defined direct-write noncontact technologies, such as ink-jet printing, for deposition of metallic structures on various substrates. Microfabrication of such structures by a lithographic technique is a time-consuming and expensive

* To whom correspondence should be addressed. Tel: (972)-2-6584967. Fax: (972)-2-6584350. E-mail: magdassi@cc.huji.ac.il.

(1) Aiken, J. D., III; Finke, R. G. *J. Mol. Catal. A* **1999**, *145*, 1.
(2) Bönnemann, H.; Richards, R. M. *Eur. J. Inorg. Chem.* **2001**, 2455.
(3) Schmid, G. *Adv. Eng. Mater.* **2001**, *3*, 737.
(4) Feldheim, D. L.; Foss, C. A., Jr. In *Metal Nanoparticles: Synthesis, Characterization and Applications*; Feldheim, D. L., Foss, C. A., Jr., Eds.; Marcel Dekker: New York, 2002; Chapter 1, p 1.
(5) Buffat, P.; Borel, J. P. *Phys. Rev. A* **1976**, *13*, 2287.
(6) Creighton, J. A. In *Surface Enhanced Raman Scattering*; Chang, R. K., Furtak, T. E., Eds.; Plenum Press: New York, 1982; Chapter 12, p 315.
(7) Lue, J.-T. *J. Phys. Chem. Solids* **2001**, *62*, 1599.
(8) Kelly, K. L.; Jensen, T. R.; Lazarides, A. A.; Schatz, G. C. In *Metal Nanoparticles: Synthesis, Characterization and Applications*; Feldheim, D. L., Foss, C. A., Jr., Eds.; Marcel Dekker: New York, 2002; Chapter 4, p 89.
(9) Johnson, R. C.; Hupp, J. T. In *Metal Nanoparticles: Synthesis, Characterization and Applications*; Feldheim, D. L., Foss, C. A., Jr., Eds.; Marcel Dekker: New York, 2002; Chapter 6, p 141.
(10) Natan, M. J.; Lyon, L. A. In *Metal Nanoparticles: Synthesis, Characterization and Applications*; Feldheim, D. L., Foss, C. A., Jr., Eds.; Marcel Dekker: New York, 2002; Chapter 8, p 183.
(11) Forster, S.; Antonietti, M. *Adv. Mater.* **1998**, *10*, 195.
(12) Moffit, M.; Eisenberg, A. *Chem. Mater.* **1995**, *7*, 1178.
(13) Ghosh, K.; Maiti, S. N. *J. Appl. Polym. Sci.* **1996**, *60*, 323.
(14) Andres, R. P.; Bielefeld, J. D.; Henderson, J. I.; Janes, D. B.; Kolagunta, V. R.; Kubiak, C. P.; Mahoney, W. J.; Osifchin, R. J. *Science* **1996**, *273*, 1960.
(15) McConnel, W.; Brousseau, L. C., III; House, A. B.; Lowe, L. B.; Tenent, R. C.; Feldheim, D. L. In *Metal Nanoparticles: Synthesis, Characterization and Applications*; Feldheim, D. L., Foss, C. A., Jr., Eds.; Marcel Dekker: New York, 2002; Chapter 13, p 319.
(16) Musick, M. D.; Keating, C. D.; Lyon, L. A.; Botsko, S. L.; Peña, D. J.; Holliway, W. D.; McEvoy, T. M.; Richardson, J. N.; Natan, M. J. *Chem. Mater.* **2000**, *12*, 2869.
(17) Korgel, B. A.; Fitzmaurice, D. *Adv. Mater.* **1998**, *10*, 661.
(18) Taleb, A.; Petit, C.; Pileni, M. P. *J. Phys. Chem. B* **1998**, *102*, 2214.

10.1021/cm021804b CCC: $25.00
Published on Web 04/24/2003

process. Techniques based on expelling small droplets of molten metals onto a substrate have met several problems, such as difficulty in adhering droplets onto a substrate, oxidation of the liquid metal, and difficulty in fabricating a droplet-expulsion mechanism compatible with high temperatures.[19−21]

Several methods for metallic image generation with the use of ink-jet technology have been described. One of them was based on ink containing a reducing agent and receiving material containing the silver salt and, in contrast, on ink and the receiving support containing a silver salt and reducer, respectively. Heating the receiving support during or after the ink deposition resulted in an image formed by silver metal.[22,23] Another method is based on ink-jet printing of organometallic precursors dissolved in organic solvent with subsequent conversion of the precursor to metal at elevated temperatures (∼300 °C).[24−27] To increase the metal (silver) loading of ink and to obtain higher decomposition rates, silver or other metal nanoparticles may be added to the ink along with the organometallic precursor. Near-bulk conductivity of printed silver films has been achieved with such compositions.[27]

Conventional pigments in ink-jet inks contain particles in the size range of 100−400 nm. In general, reducing the particle size to 50 nm or less should show improved image quality and improved printhead reliability when compared to inks containing significantly larger particles.[28] Fuller et al.[21] demonstrated ink-jet printing with the use of colloidal inks containing 5−7-nm particles of gold and silver in organic solvent, α-terpineol, to build electrically and mechanically functional metallic structures. When sintered at 300 °C, the resistivity of the printed silver structures was found to be 3 $\mu\Omega$·cm, about twice that for bulk silver.

The majority of inks in ink-jet printers are water-based inks. The use of metal nanoparticles as pigments requires the elaboration of ink formulations containing stable concentrated aqueous metal colloid. The most widely used method of silver nanoparticles preparation in an aqueous medium is chemical reduction of water-soluble silver salts by reducing agents, such as sodium and potassium borohydrides,[6,29−36] trisodium citrate,[37−40] hydrazine,[41,42] ascorbic acid,[41] hydrocarbons,[41] and gaseous hydrogen.[41] To prevent agglomeration and precipitation, a variety of substances were used to stabilize the silver colloids: amphiphilic nonionic polymers and polyelectrolytes,[41,43−52] gelatin,[34,52,53] ionic and nonionic surfactants,[29−31,54,55] polyphosphates,[43] nitrilotriacetate,[56] CS_2,[32] 3-aminopropyltrimethoxysilane,[57] amino- and carboxylate-terminated poly(amido amine) dendrimers,[58,59] and crown ethers.[60] However, the stable dispersions of silver nanoparticles, described up to now, are characterized by concentrations that amount only to 10^{-5}−10^{-2} M (about 0.0005−0.1%), even in the presence of stabilizers.[29−37,41−43,54,61−64] (It is almost impossible to obtain a stable aqueous silver colloid with the metal concentration above 10^{-3} M without an additional stabilizer, due to fast particle aggregation.[30])

Since ink-jet ink compositions contain, in addition to dyes or pigments, other additives, such as humectants, bactericides and fungicides, and binders (polymeric additives, which improve the dye or pigment binding to substrate), the stabilizers should be compatible with these substances and should not change noticeably the physicochemical and rheological characteristics of inks.

The present research focused on the preparation and characterization of stabilized concentrated silver nanocolloids, which can be used further as pigments in ink-jet inks. Sodium salt of carboxymethyl cellulose was

(19) Priest, J.; Jacobs, E.; Smith, C., Jr.; DuBois, P.; Holt, B.; Hammerschlag, B. *Int. J. Microcircuits Electron. Packag.* **1994**, *17*, 219.
(20) Hayes, D. J.; Cox, W. R.; Grove, M. E. *J. Electron. Manuf.* **1998**, *8*, 209.
(21) Fuller, S. B.; Wilhelm, E. J.; Jacobson, J. M. *J. Microelectromech. Syst.* **2002**, *11*, 54.
(22) Leenders, L.; Oelbrandt, L.; Van der Bogaert, J.; Desie., G. U.S. Patent 5,501,150, 1996.
(23) Leenders, L.; Uyttendaele, C.; Uytterhoeven, H. U.S. Patent 5,621,449, 1997.
(24) Vest, R. W.; Tweedell, E. P.; Buchanan, R. C. *Int. J. Hybrid Microelectron.* **1983**, *6*, 261.
(25) Teng, K. F.; Vest, R. W. *IEEE Trans. Ind. Electron.* **1988**, *35*, 407.
(26) Teng, K. F.; Vest, R. W. *IEEE Electron. Device Lett.* **1988**, *9*, 591.
(27) Curtis, C.; Rivkin, T.; Miedaner, A.; Alleman, J.; Perkins, J.; Smith, L.; Ginley, D. *Proceedings of the NCPV Program Review Meeting*, Lakewood, CO, Oct 14−17, 2001; The National Center for Photovoltaics: Golden, CO, p 249.
(28) Bermel, A. D.; Bugner, D. E. *J. Imaging Sci.* **1999**, *43*, 320.
(29) Pal, T.; Sau, T. K.; Jana, N. R. *Langmuir* **1997**, *13*, 1481.
(30) Wang, W.; Efrima, S.; Regev, S. *Langmuir* **1998**, *14*, 602.
(31) Wang, W.; Chen, X.; Efrima, S. *J. Phys. Chem. B* **1999**, *103*, 7238.
(32) Jiang, X.; Xie, Y.; Lu, J.; Zhu, L.; He, W.; Qian, Y. *Langmuir* **2001**, *17*, 3795.
(33) Creighton, J. A.; Blatchford, C. G.; Albrecht, M. G. *J. Chem. Soc., Faraday 2* **1979**, *75*, 790.
(34) Kamyshny, A. L.; Zakharov, V. N.; Fedorov, Yu. V.; Galashin, A. E.; Aslanov, L. A. *J. Colloid Interface Sci.* **1993**, *158*, 171.
(35) Sánchez-Cortés, S.; Garcia-Ramos, J. V.; Morcillo, G. *J. Colloid Interface Sci.* **1994**, *167*, 428.
(36) Cliffel, D. E.; Zamborini, F. P.; Gross, S. M.; Murray, R. W. *Langmuir* **2000**, *16*, 9699.
(37) Lee, P. C.; Meisel, D. *J. Phys. Chem.* **1982**, *86*, 3391.
(38) Hildebrandt, P.; Stockburger, M. *J. Phys. Chem.* **1984**, *88*, 5935.
(39) Bright, R. M.; Musick, M. D.; Natan, M. J. *Langmuir* **1998**, *14*, 5695.
(40) Munro, C. H.; Smith, W. E.; Garner, M.; Clarkson, J.; White, P. C. *Langmuir* **1995**, *11*, 3712.
(41) Esumi, K.; Ishizuki, N.; Torigoe, K.; Nakamura, H.; Meguro, K. *J. Appl. Polym. Sci.* **1992**, *44*, 1003.
(42) Nickel, U.; zu Castell, A.; Pöppl, K.; Schneider, S. *Langmuir* **2000**, *16*, 9087.
(43) Henglein, A. *Chem. Mater.* **1998**, *10*, 444.
(44) Mayer, A. B. R. *Polym. Adv. Technol.* **2001**, *12*, 96.
(45) Yonezawa, Y.; Kijima, M.; Sato, T. *Ber. Bunsen-Ges. Phys. Chem.* **1992**, *96*, 1828.
(46) Zhao, X. K.; Fendler, J. H. *J. Phys. Chem.* **1990**, *94*, 3384.
(47) Fendler, J. H.; Meldrum, F. C. *Adv. Mater.* **1995**, *7*, 607.
(48) Quaroni, L.; Chumanov, G. *J. Am. Chem. Soc.* **1999**, *121*, 10642.
(49) Huang, H. H.; Ni, X. P.; Loy, G. L.; Chew, C. H.; Tan, K. L.; Loh, F. C.; Deng, J. F.; Xu, G. Q. *Langmuir* **1996**, *12*, 909.
(50) Meguro, K.; Nakamura, Y.; Hayashi, Y.; Torizuka, M.; Esumi, K. *Bull. Chem. Soc. Jpn.* **1988**, *61*, 347.
(51) Kapoor, S.; Gopinathan, C. *Radiat. Phys. Chem.* **1997**, *49*, 51.
(52) Kapoor, S. *Langmuir* **1996**, *12*, 1021.
(53) Kapoor, S.; Lawless, D.; Kennepohl, P.; Meesel, D.; Serpone, N. *Langmuir* **1994**, *10*, 3018.
(54) Liz-Marzán, L. M.; Lado-Touriño, I. *Langmuir* **1996**, *12*, 3585.
(55) Chen, Y.-H.; Yeh, C.-S. *Colloids Surf. A* **2002**, *197*, 133.
(56) Zhu, J.; Liu, S.; Palchik, O.; Koltypin, Y.; Gedanken, A. *Langmuir* **2000**, *16*, 6396.
(57) Pastoriza-Santos, I.; Liz-Marzán, L. M. *Langmuir* **1999**, *15*, 948.
(58) Kéki, S.; Török, J.; Deák, G.; Daróczi, L.; Zsuga, M. *J. Colloid Interafce Sci.* **2000**, *229*, 550.
(59) Manna, A.; Imae, T.; Aoi, K.; Okada, M.; Yogo, T. *Chem. Mater.* **2001**, *13*, 1674.
(60) Jao, T.-C.; Beddard, G. S.; Tundo, P.; Fendler, J. H. *J. Phys. Chem.* **1981**, *85*, 1963.
(61) Lee, N.-S.; Sheng, R.-S.; Morris, M. D.; Schopfer, L. M. *J. Am. Chem. Soc.* **1986**, *108*, 6179.
(62) Van Hyning, D. L.; Zukoski, C. F. *Langmuir* **1998**, *14*, 7034.
(63) Henglein, A.; Giersig, M. *J. Phys. Chem. B* **1999**, *103*, 9533.
(64) Van Hyning, D. L.; Klemperer, W. G.; Zukoski, C. F. *Langmuir* **2001**, *17*, 3128.

used as a stabilizer, which also functions as a binder for ink-jet inks.

Experimental Section

Materials. $AgNO_3$ (SigmaUltra, >99%) and carboxymethyl cellulose (CMC) were purchased from Sigma Chemical Co. Wetting and dispersing agents Disperbyk-181 and Disperbyk-184 for ink preparation were purchased from BYK-Chemie (Germany). All other reagents were of analytical grade. All solutions were prepared with the use of triply distilled water.

Silver Nanoparticles Preparation. The nanoparticles were prepared by reduction of $AgNO_3$ with trisodium citrate at various concentrations of reagents according to the procedure described by Lee and Meisel.[37] (The $AgNO_3$:citrate molar ratio was kept constant, 1.37.)

The preparation of silver nanoparticles without a stabilizer was performed as follows. Two milliliters of trisodium citrate solution in water (1−10%) was added dropwise to a heated (94−95 °C) solution of $AgNO_3$ (18−180 mg in 100 mL of water) while stirring. The mixture was kept heated for 10 min, and then it was cooled to room temperature.

The preparation of stabilized Ag nanoparticles was performed as follows. Two milliliters of trisodium citrate solution (1−10%) in aqueous CMC (0.025−0.2%) was added dropwise to a heated (94−95 °C) solution of $AgNO_3$ (18−180 mg in 100 mL of aqueous CMC with concentration 0.025−0.2%) while stirring. The mixture was kept heated for 10 min, and then it was cooled to room temperature. If not otherwise stated, a "low-viscosity" CMC (average M.W. 90000, viscosity of 4% aqueous solution 50−200 cP at 25 °C, 6.5−9 carboxymethyl groups per 10 anhydroglucose units) was used.

The highly concentrated dispersions of silver nanoparticles were prepared by partial or exhausted lyophilization of the stabilized nanocolloids followed by redispersion in a proper amount of water.

Dynamic Light Scattering (DLS). The *Z*-average mean particle size (Z_{ave}) was measured by dynamic light scattering with a Zetasizer 3000 (external Ar^+ laser, wavelength 488 nm, power 70 mW, or internal He−Ne laser, wavelength 633, power 10 mW; detector angle 90°; temperature 25 °C) and with HPPS (He−Ne laser, wavelength 633, power 10 mW), both instruments of Malvern Instruments, UK. The Z_{ave} was taken as a mean value of three to four measurements.

Particle Size Measurement by Time-of-Transition Method (TTM). Size of particles larger than 0. 5 μm was measured by a Galai CIS-1 particle analyzer (Galai, Israel) based on time-of-transition theory. A He−Ne laser beam is scanned circularly by a rotating wedge prism and focused down to a 1.2-μm spot, which scans the sample measurement volume. As the particles within that sample volume are individually bisected by the laser spot, interaction signals are generated and are then detected by a PIN photodiode. Since the beam rotates at a constant speed, the duration of interaction provides a direct measurement of each particle's size. The particle size was taken as a mean value of three to four measurements.

Zeta Potential Measurements. The ζ potential is related to the electrophoretic mobility by the Henry equation

$$U_E = 2\epsilon\zeta\, f(\kappa a)/3\eta$$

where ζ is the zeta potential, U_E is the electrophoretic mobility, ϵ is the dielectric constant, η is the viscosity, and $f(\kappa a)$ is the factor including electric double-layer thickness and particle diameter. The electrophoretic determinations of ζ potentials were made in aqueous media at moderate electrolyte concentration, and $f(\kappa a)$ in this case is 1.5. This is the value used in the Smoluchowski approximation:

$$U_E = \epsilon\zeta/\eta$$

The ζ potentials were determined by a Zetasizer 3000 (internal He−Ne laser) and taken as a mean value from three to four measurements.

Viscosity Measurements. Viscosity of Ag colloids was measured with a Cannon-Fenske (reverse flow) viscometer. It was found that the viscosity of the stabilized silver colloids increases linearly from 1 to 2.4 cP with the increase in CMC concentration from 0.05 to 0.5 wt %. In all measurements of the particle size by DLS as well as ζ potentials, the changes in viscosity caused by CMC addition were taken into account.

Transmission Electron Microscopy (TEM). Samples were prepared by placing a drop of the Ag dispersion on a carbon-coated Formvar Cu grid, 300 mesh, for 2 min. Then water was removed by filter paper and samples were examined with a Philips Tecnai 211 microscope operating at 100 kV.

X-ray Diffraction (XRD). The diffraction was performed on the powder obtained after lyophilization of the silver nanoparticles dispersion with a PW 1710 diffractometer with a Cu tube anode.

Visible−UV Spectrophotometry. Spectra of Ag colloids were recorded with the use of an Hitachi double-beam spectrophotometer U-2000.

Stability Measurement. Stability of silver colloids was evaluated by measuring the change in particle size with time at room temperature.

Ink-Jet Printing. For testing the silver-based inks, a piezoelectric Drop-on-Demand ink-jet Epson Stylus Color 460 printer was used. The ink formulation containing silver nanoparticles as a pigment was placed in a standard ink cartridge and printed onto two substrates: paper (resolution 720 dpi) and ink-jet transparency (resolution 360 dpi).

Results and Discussion

Formation and Stabilization of Silver Nanoparticles. To identify the nature of nanoparticles, X-ray diffraction was performed on the powder of unstabilized and stabilized (0.2 wt % of CMC) colloids, which were lyophilized immediately after preparation ([Ag] = 0.04 wt %). The reflection peaks characteristic of Ag^0 were found in both samples and indexed as 111 (d[Å] = 2.359 and 2.357), 200 (d[Å] = 2.042 and 2.046), and 220 (d[Å] = 1.447 and 1.443, respectively), indicating that the product is silver with cubic symmetry. Analogous data were obtained by Jiang et al.[32] with the use of KBH_4 as a reducing agent. The electron diffraction patterns (data not shown) of silver nanoparticles show concentric circles due to random orientation of crystal planes. The radii of crystalline rings are consistent with the XRD data.

While using nanocolloids with silver concentrations above 10^{-3} M, it was impossible to obtain stable preparation without the use of additional stabilizer. For example, precipitation of silver from a 2×10^{-3} M silver nanocolloid was observed within a few days after preparation, while 10^{-3} M nanocolloid precipitates in about 3 weeks. Figure 1 shows the effect of increasing silver concentration on the average particle size in the absence of additional stabilizer, 1 h after preparation. It is apparent that at concentrations higher than 6×10^{-3} M the particle size increases rapidly, and a precipitate forms practically immediately after preparation.

In general, we found that the use of CMC as a stabilizer results in the formation of stable dispersions of silver nanoparticles and that a CMC having average molecular weight of 90000 and 6.5−9 carboxymethyl groups per 10 anhydroglucose units favors the formation of the smallest silver nanoparticles compared to the

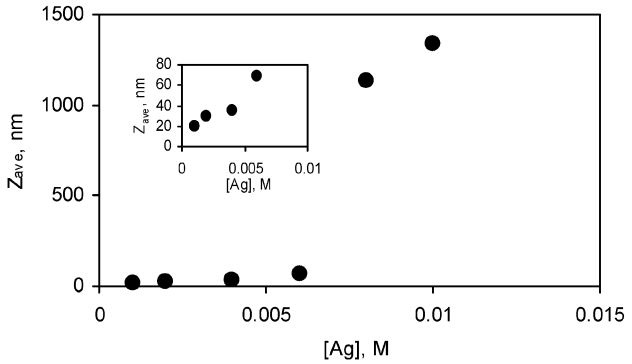

Figure 1. Average particle size as a function of Ag concentration for unstabilized colloid (measurements were carried out by DLS and TTM 1 h after preparation).

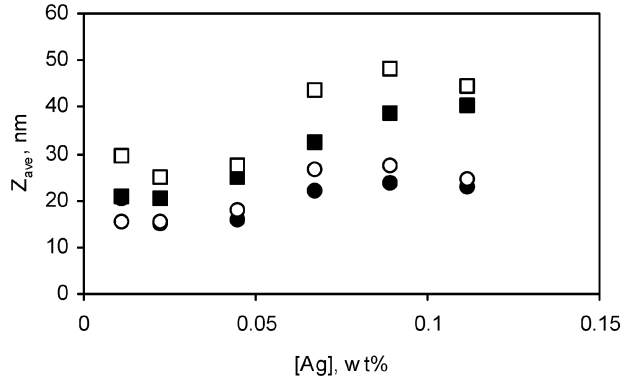

Figure 2. Average particle size as a function of Ag concentration for freshly prepared silver hydrosols at different concentrations of CMC by DLS: (●) 0.025 wt %; (○) 0.05 wt %; (■) 0.1 wt %; (□) 0.2 wt %.

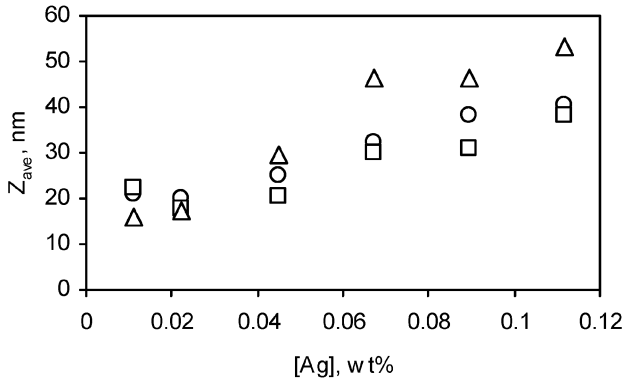

Figure 3. Average particle size as a function of Ag concentration and time at a CMC concentration of 0.1 wt % by DLS: (○) 1 day; (□) 13 days; (△) 60 days.

other types of CMC (data not presented). All experiments presented in this paper were carried out with this type of CMC.

It was found that the concentration of CMC affects the average size of the silver nanoparticles, but in the range of CMC concentrations of 0.025−0.2 wt %, the average particle size does not exceed 50 nm (Figure 2).

The stabilization of silver nanoparticles prepared in the presence of CMC was evaluated by size measurements for samples stored at room temperature (Figure 3). Only a slight increase in the average particle size with time was observed, and the size does not exceed 60 nm even after 2 months.

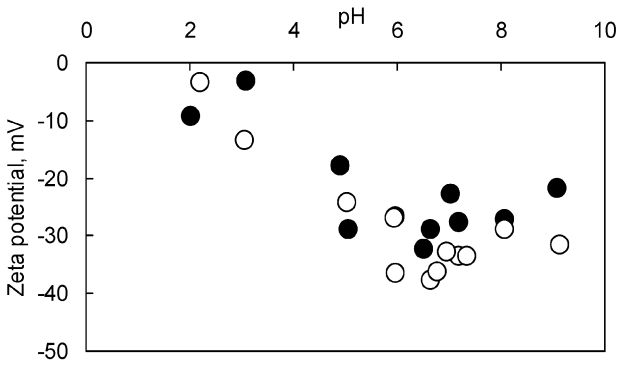

Figure 4. Zeta potential of silver nanoparticles as a function of pH ([Ag] = 10^{-3} M). (●) unstabilized colloid; (○) CMC-stabilized colloid ([CMC] = 0.2 wt %).

To evaluate the contribution of electrostatic repulsion to the silver nanoparticles stability, we measured the ζ potential as a function of pH. As seen from Figure 4, both unstabilized and CMC-stabilized silver nanoparticles are negatively charged in the whole pH range studied (from 2 to 9). The negative value of ζ potential is almost constant in the pH range of 6−8 (−27 ± 5 mV for unstabilized and 33 ± 5 mV for CMC-stabilized colloids, respectively), but is noticeably lower at pH < 4. The negative charge of the unstabilized silver nanoparticles is related to the citrate ions adsorption on the particle surface. At pH higher than 3.07 (pK_{a1} of citric acid) and lower than 4.77 (pK_{a2}), citric acid has one negative charge; a further increase in pH results in the dissociation of the second carboxylic group. At pH > 5.6 (pK_{a3}) citric acid possesses three negative charges. Previously published data[65,66] also reported the negative charge of the silver nanoparticles prepared by the citrate method. Frens and Overbeek[67] have found even much more negative ζ potential (−80 ± 5 mV) and have explained this value by "superequivalent" specific adsorption of citrate ions onto nanoparticles. A more negative value of ζ potential for CMC-stabilized nanoparticles in the pH range of 6−8, as compared with unstabilized nanoparticles, can be explained by the contribution of the negatively charged polymeric moieties (the CMC molecule is negatively charged at pH > 4.3).

Characteristics of Dispersions of Silver Nanoparticles. In general, unstabilized colloids appeared yellow with brownish tint, while CMC-stabilized colloids have brown-reddish color in transmitted light. The spectra of all colloids (Figure 5) are typical of those for hydrosols of silver nanoparticles prepared by reduction with sodium citrate[37−40,68−70] and are characterized by asymmetric absorption bands with maxima at 417−440 nm and two distinct shoulders at 350−352 and 380−382 nm. (The only exception is CMC-stabilized 10^{-2} M colloid, which has an absorption maximum at 399 nm

(65) Heard, S. M.; Grieser, F.; Barraclough, C. G.; Sanders, J. V. *J. Colloid Interface Sci.* **1983**, *93*, 545.
(66) Ung, T.; Griersig, M.; Dunstan, D.; Mulvaney, P. *Langmuir* **1997**, *13*, 1773.
(67) Frens, G.; Overbeek, J. Th. G. *Kolloid Z. Z. Polym.* **1969**, *233*, 922.
(68) Rivas, L.; Sanchez-Cortes, S.; Garcia-Ramos, J. V.; Morcillo, G. *Langmuir* **2001**, *17*, 574.
(69) Fornasiero, D.; Grieser, F. *J. Chem. Phys.* **1987**, *87*, 3213.
(70) Fornasiero, D.; Grieser, F. *J. Colloid Interface Sci.* **1991**, *141*, 168.

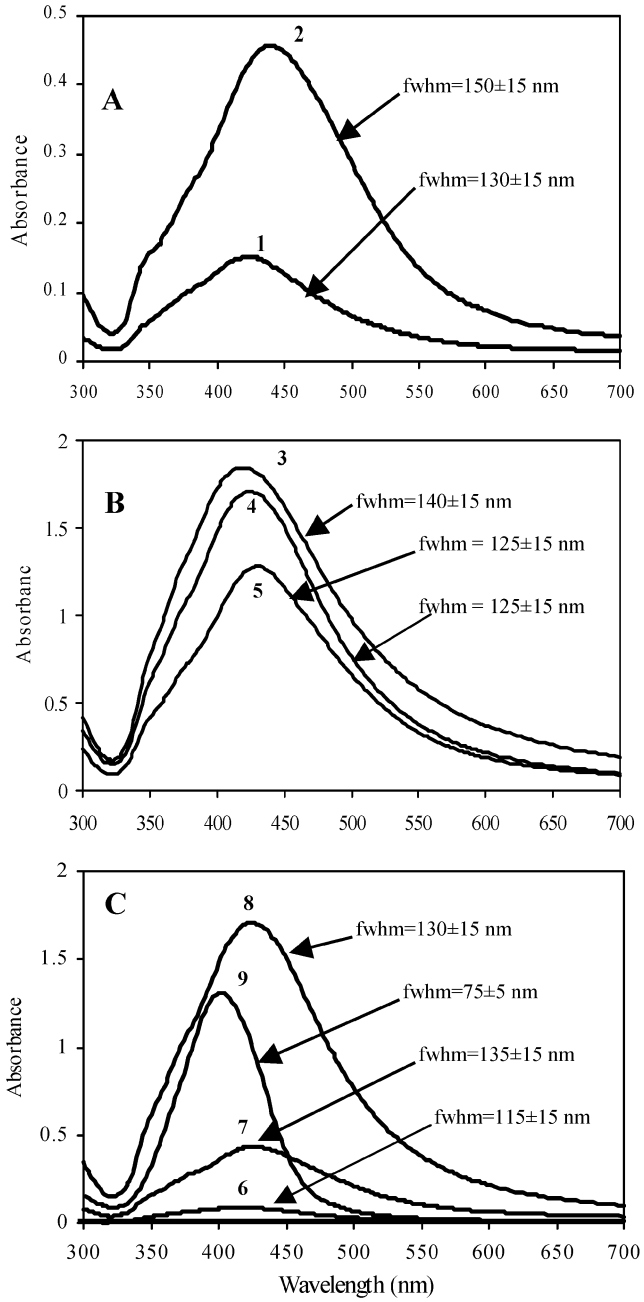

Figure 5. Absorption spectra of freshly prepared silver colloids. A: unstabilized colloids, [Ag] = 10^{-3} M (1) and 2 × 10^{-3} M (2). B: CMC-stabilized colloids, [Ag] = 4 × 10^{-3} M, CMC concentrations of 0.025 wt % (3), 0.1 wt % (4), and 0.2 wt % (5). C: CMC-stabilized colloids, [CMC] = 0.1 wt %, Ag concentrations of 10^{-3} M (6), 2 × 10^{-3} M (7), 4 × 10^{-3} M (8), and 10^{-2} M (9). All samples were diluted 10 times before recording the spectra with the exception of sample (9), which was diluted 100 times.

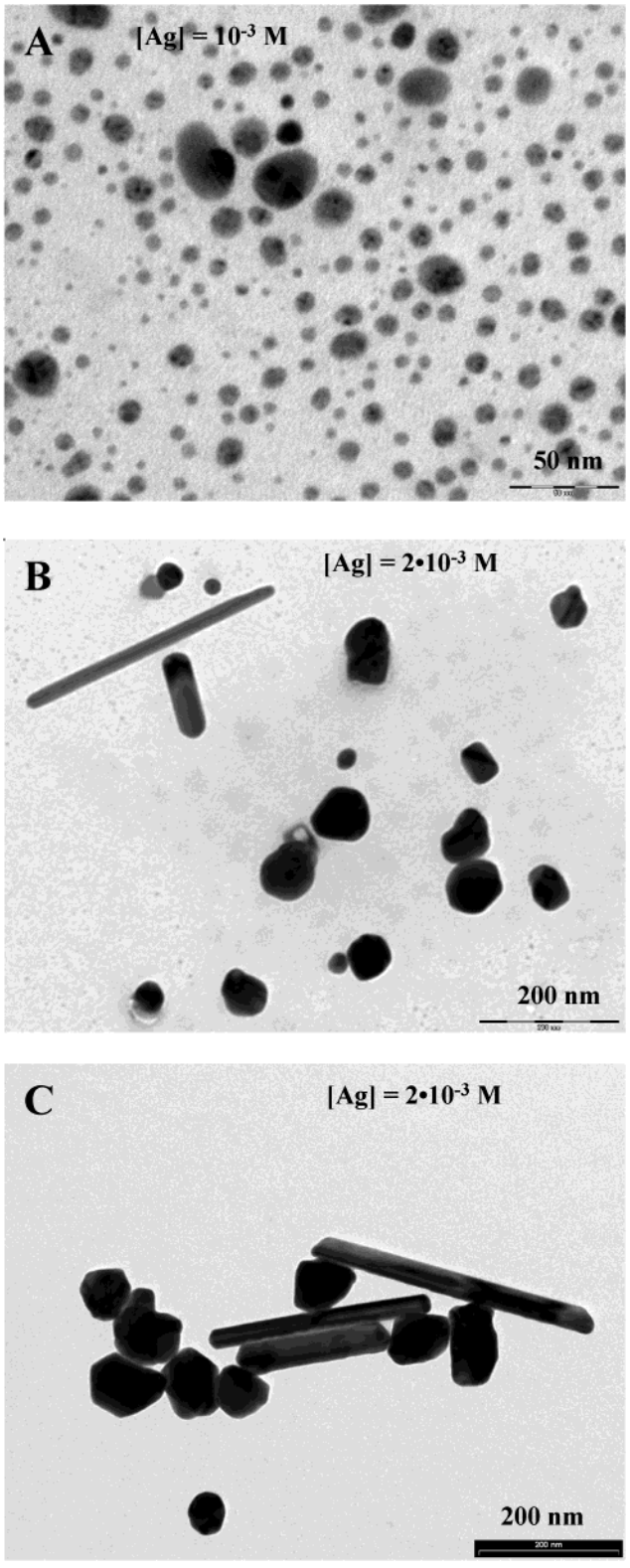

Figure 6. TEM micrographs of unstabilized silver nanoparticles. A: [Ag] = 10^{-3} M. B and C: [Ag] = 2 × 10^{-3} M (different grids).

and shows no shoulders.) An intense absorption peak around 400 nm is attributed to the surface plasma excitation of silver nanoparticles (dipolar surface plasmon band).[33,40,49,71,72] According to Kerker,[72] the "true" position of the surface plasmon band for spherical silver nanoparticles in water is 382 nm. The reason for the variable absorption spectra is the existence of adsorption and electronic coupling with the solvent.[71] The general trend is also that the absorption peak shifts toward longer wavelengths as particles become larger.[49,65,73,74] Therefore, the shoulder at ~380 nm (Figure 5) may be attributed to small (<20 nm) isolated spherical nano-

(71) Mulvaney, P. *Langmuir* **1996**, *12*, 788.
(72) Kerker, M. *J. Colloid Interface Sci.* **1985**, *105*, 297.
(73) Mie, G. *Ann. Phys.* **1908**, *25*, 377.
(74) Wang, D. S.; Kerker, M.; Chew, H. *Appl. Opt.* **1890**, *19*, 2135.

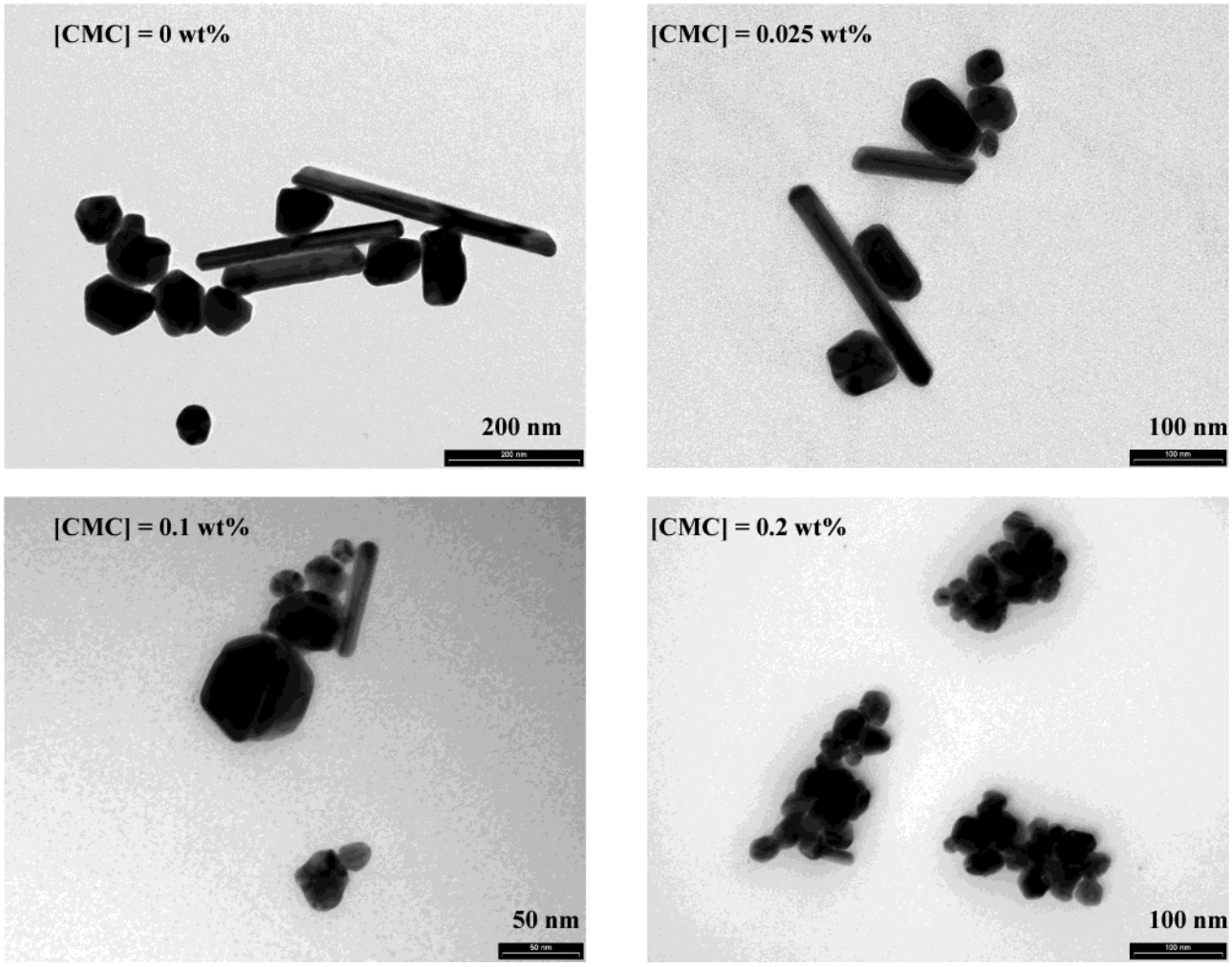

Figure 7. TEM micrographs of CMC-stabilized silver nanoparticles at different concentrations of CMC ([Ag] = 4×10^{-3} M).

particles. The appearance of the shoulder at ~350 nm may be explained by both the nonspherical shape of a portion of particles and by the presence of doublets and linear aggregates. It has been shown by Kerker[72] that, for randomly oriented prolate or oblate ellipsoids or linear aggregates of spherical nanoparticles, the absorption band splits into two bands, the high energy band being localized at ~350 nm. Analogous results were obtained by Fornasiero and Grieser,[69,70] who carried out the deconvolution of the experimental absorption spectra of citrate-reduced silver nanoparticles into a set of Gaussian bands and found out that the monomer band, under certain conditions, may be flanked on each side by aggregate bands (at low level of aggregation), one at high energy (~360 nm) and two at low energy (~530 and 480 nm). Higher levels of aggregation result usually in the appearance of a broad band at high wavelength (~530 nm). We did not observe this high wavelenth band in the spectra of both unstabilized and stabilized colloids.

It has been shown that the matrix effect of the stabilizing polymer may strongly influence the position, intensity, width, and shape of the absorption band.[43,49,66] We found that the peak wavelength increasingly shifts from 419 ± 1 to 424 ± 1 and 430 ± 1 nm with an increase in CMC concentration from 0.25 to 0.1 and 0.2 wt %, respectively, at a silver concentration of 4×10^{-3} M (Figure 5B). Ung et al.[66] have also reported that the initial surface plasmon band of the colloidal silver shifted to the red with an increase in the concentration of poly(acrylic acid) as a stabilizer. This effect was attributed to the creation of a dielectric coating around the particles, resulting in a change in the refractive index in their vicinity. For example, a shift of 10 nm for the surface plasmon peak was found to correspond to a shell layer with a refractive index of 1.5 having a thickness of about 10−14 Å.[66] Another effect of the increase in the stabilizer concentration is the decrease in the peak intensity at constant silver concentration (Figure 5B). This result may be explained by a larger size of particles or their aggregates at higher concentrations of CMC. In general, upon aggregation, the peak attributed to the monomeric particles decreases in size.[65,70] It has also been found that the adsorption of complexing ions (in our case, CMC carboxylate anions) onto colloidal silver results in strong damping of the surface plasmon absorption band.[71]

The full width of the absorption band at half-maximum (fwhm), which can be used as a criterion of polydispersity,[31,40] is high (115−150 nm) for all colloids (Figure 5). The only exception is a CMC-stabilized colloid with Ag concentration as high as 10^{-2} M (Figure 5C). In addition to the blue shift to 399 nm, the absorption band of this colloid becomes symmetric with a fwhm of only 75 nm, indicative of moderately monodisperse small silver nanoparticles. The size distribution

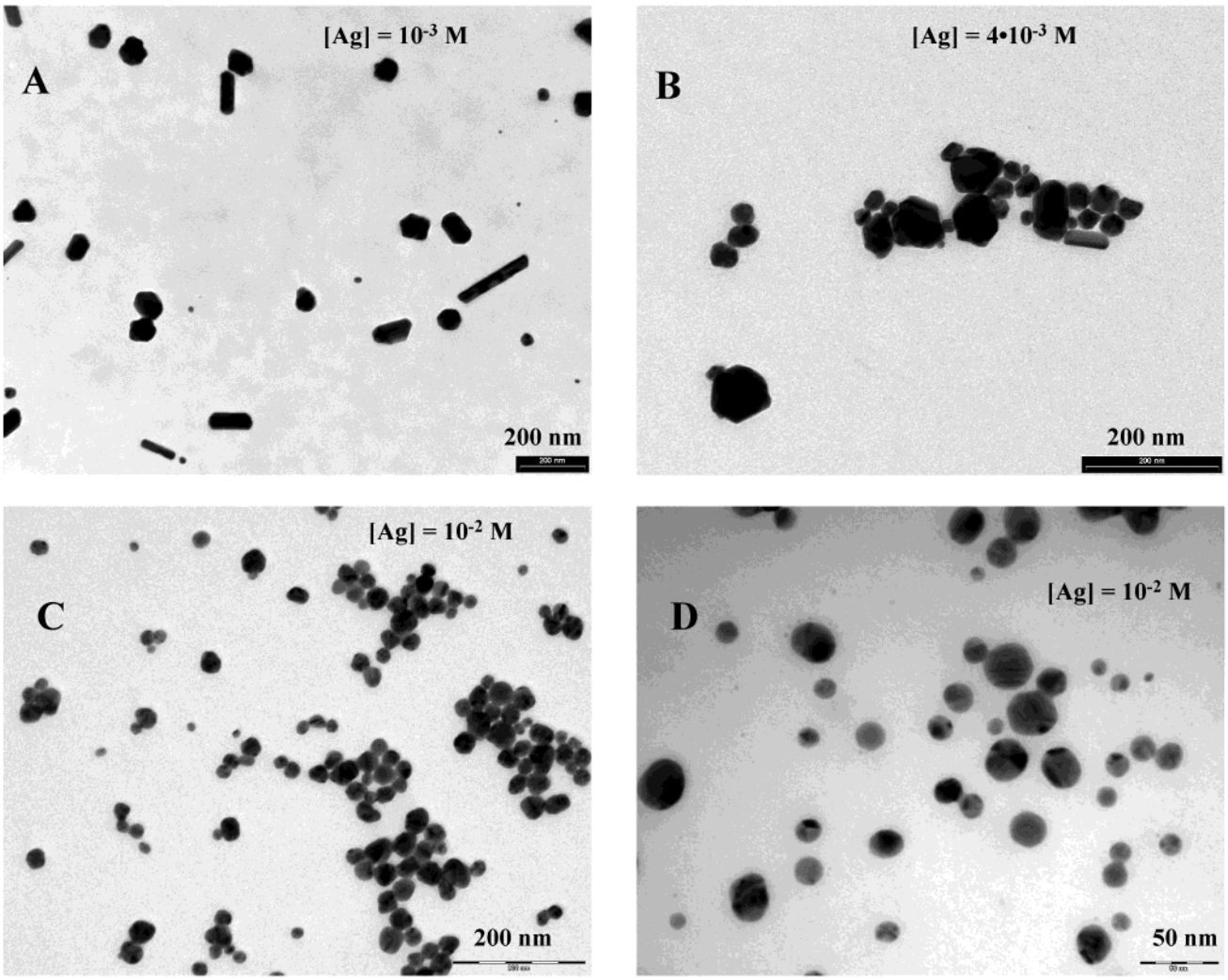

Figure 8. TEM micrographs of CMC-stabilized silver nanoparticles at different concentrations of silver. [CMC] = 0.025 wt % (A, B, C) and 0.1 wt % (D).

of colloidal dispersion of solid particles is determined by the ratio between the rates of nucleation of the solid cores, their subsequent growth, and aggregation. As the initial concentrations of reagents ($AgNO_3$ and sodium citrate) are high, a large number of nuclei are quickly generated, consuming a major fraction of the metal species in the system and resulting in the formation of small nanoparticles with relatively uniform size distribution.

In general, a wide distribution of particle size is a distinguishing feature of silver colloids prepared by citrate reduction. A variety of shapes, from spheres and cubes to rods and needles with a lengths of 180−200 nm and even 1000 nm have been observed in such colloids.[38,39,68,75] Our TEM data support these findings and is in agreement with the spectral data. As seen in Figure 6, unstabilized colloid with a silver concentration of 10^{-3} M consists of small nanoparticles of spherical and ellipsoidal shapes with very wide size distributions (from 3 to 4 to 35 nm). A twofold increase in the silver concentration results in the formation of particles of different shapes: almost spherical, rods, and particles close to hexagons. The average size of spheres and hexagons is ∼70 nm. The rods of diameter ∼20−30 nm reach 400-nm length (Figures 6B,C). Another important feature of the colloid with silver concentration of 2×10^{-3} M is a distinct observation of aggregates of particles.

In general, preparation of the silver colloid in the presence of various concentrations of the stabilizer, CMC, does not change the general regularity: a variety of shapes, including rods and agglomerates, are observed (Figures 7 and 8A,B). However, an increase in the silver concentration up to 10^{-2} M results in the formation of spherical particles with much more uniform size distribution, and the average diameter is ∼20−25 nm (Figure 8C,D). This finding correlates with noticeable narrowing of the absorption band corresponding to the surface plasmon resonance at the same silver concentration (Figure 5C).

Concentrated Dispersions of Silver Nanoparticles. To prepare dispersions with high silver concentration (>1 wt %), the CMC-stabilized nanoparticles with silver concentration ∼0.1% were lyophilized either partially to reduce the water content in the dispersion or exhaustively up to complete removal of water. In the second case, the obtained powder was redispersed in a low volume of water. Figure 9A presents the average particle size as a function of increasing silver concentra-

(75) Zhang, P. X.; Fang, Y.; Wang, W. N.; Ni, D. H.; Fu, S. Y. *J. Raman Spectrosc.* **1990**, *21*, 127.

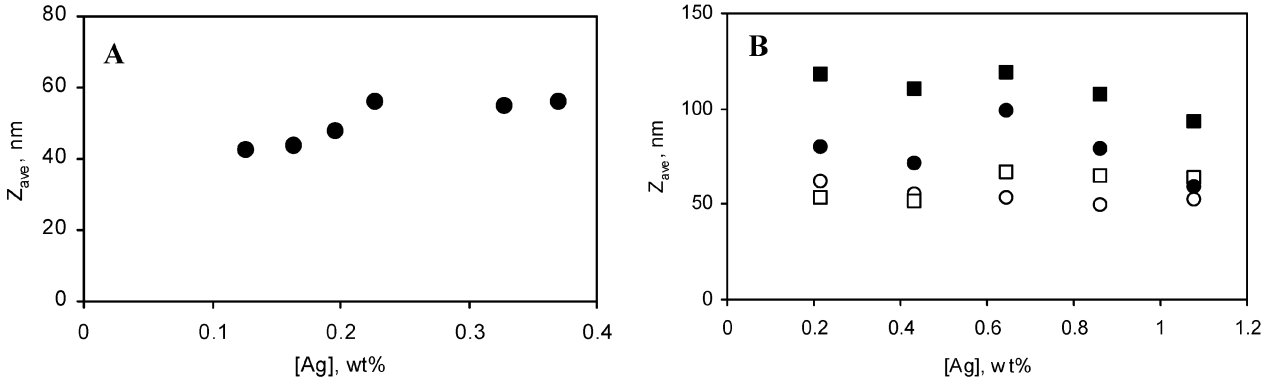

Figure 9. Average particle size as a function of Ag concentration in the process of lyophilization (A) and as a function of Ag concentration and storage time after redispersion of lyophilized Ag powder in various amounts of water (B) by DLS: (○) 1 day; (□) 12 days; (●) 48 days; (■) 205 days. Initial concentrations (before lyophilization): [Ag] = 0.1%; [CMC] = 0.1%.

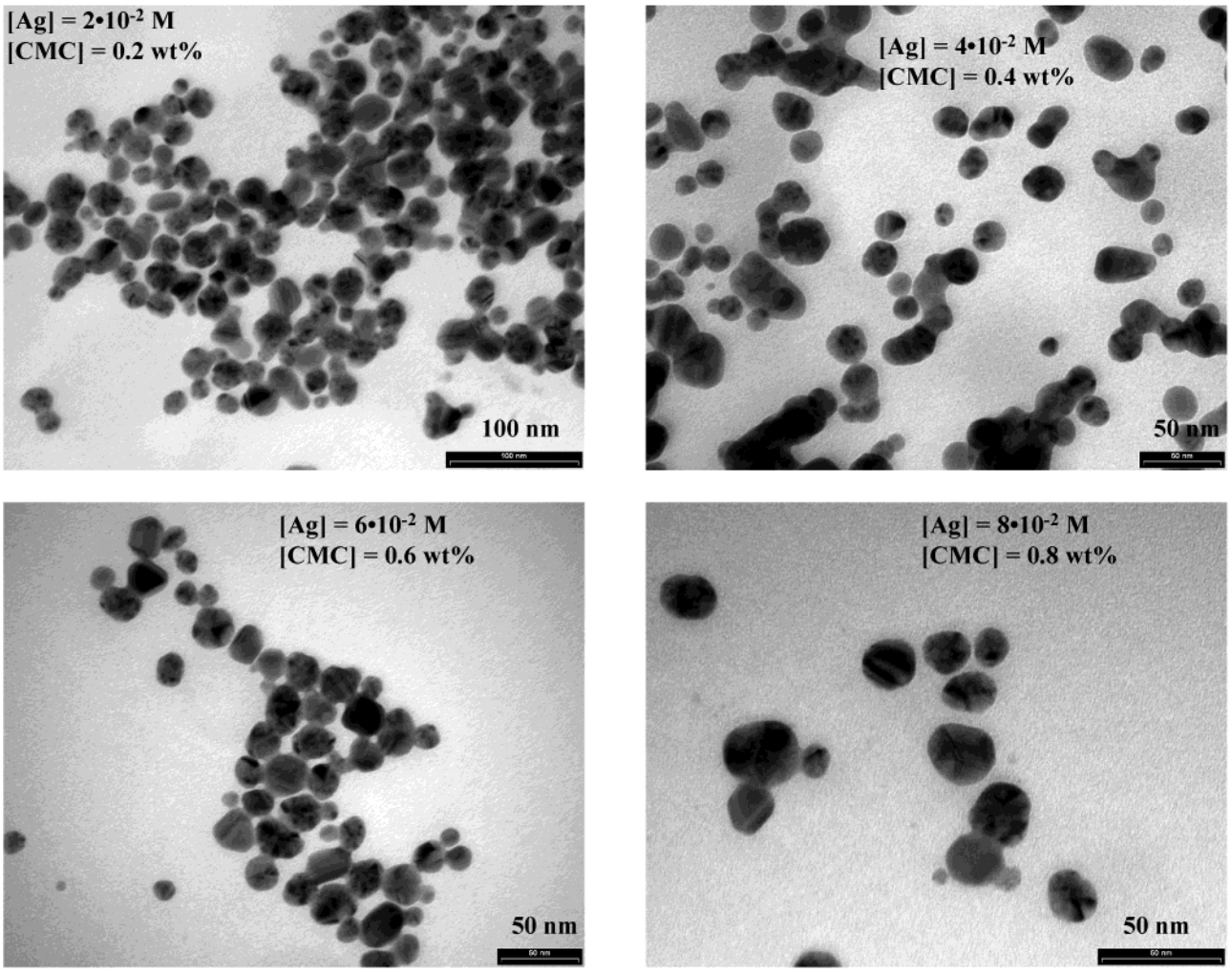

Figure 10. TEM micrographs of silver nanoparticles after redispersion of lyophilized samples. The concentrations of Ag and CMC in final redispersed samples are pointed out in micrographs.

tion during lyophilization (these concentrations were calculated according to the change in the volume of sample). It is obvious that when the lyophilization procedure is used, dispersions with a silver concentration as high as 0.37 wt % (~3.5×10^{-2} M) and particle size not exceeding 60 nm can be obtained. Colloids prepared by redispersion of a powder of silver nanoparticles obtained after lyophilization also have the average particle size of 40−70 nm, up to silver concentration of 1.1 wt % (~0.1 M). Figure 10 presents the TEM images of redispersed silver nanoparticles 1 day after preparation. In all micrographs agglomerates of loosely packed primary spherical particles with an average size of about 20−25 nm are observed. Greater values found out by DLS (Figure 9) can be explained by the greater hydrodynamic size of the CMC-enveloped particles as compared with the size evaluated by TEM. In general, it was found that the concentrated dispersions were very stable (Figure 9B), and after 205 days of storage at room temperature the particle size increases only up to 90−

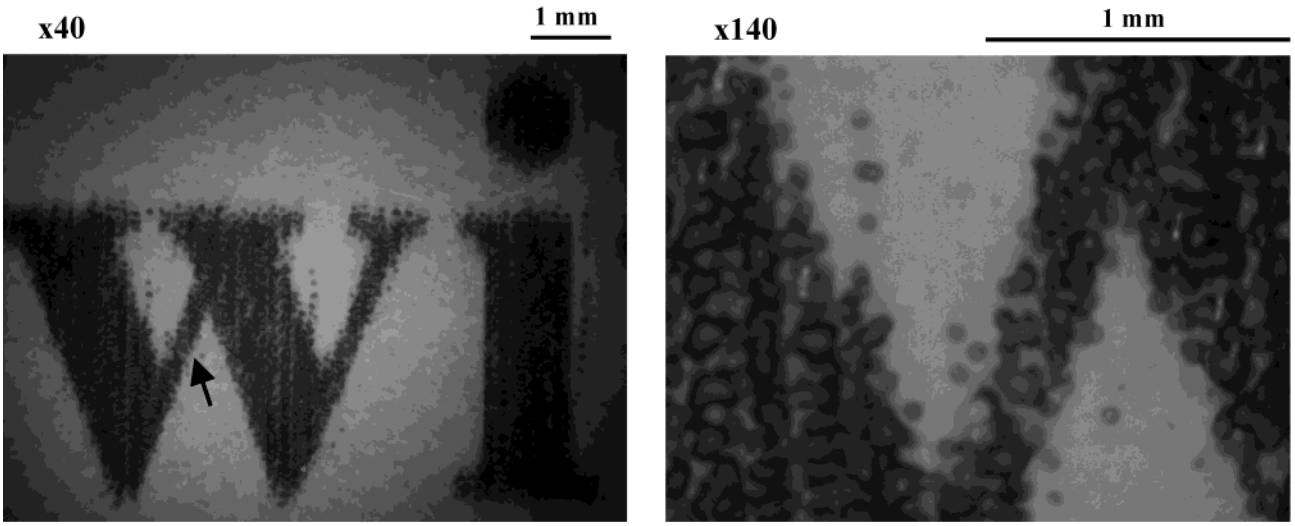

Figure 11. Images (magnifications ×40 and ×140) printed on ink-jet transparency with the use of the ink formulation containing 1 wt % of Ag, 0.2 wt % of CMC, 1 wt % of Disperbyk-184, and 0.1 wt % of Disperbyk-181. The images were taken with the use of Micro-Eye MS-222Net (NikkoEnergy).

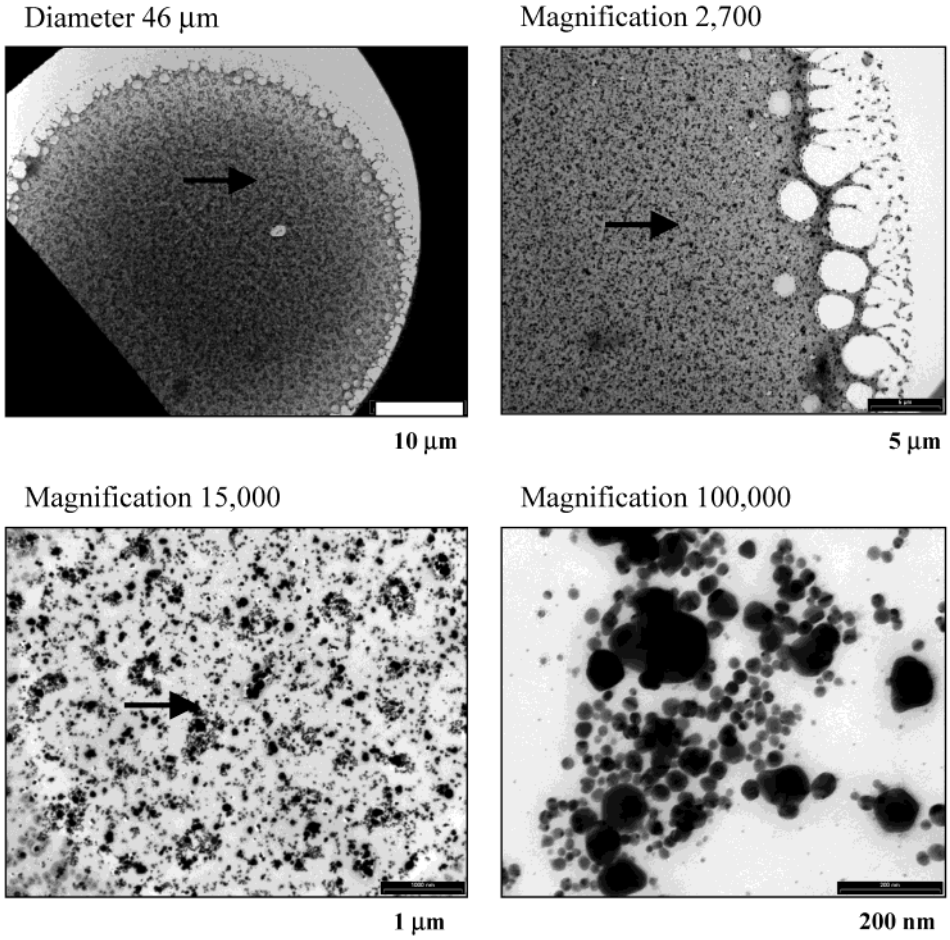

Figure 12. TEM images of the single-dot pattern printed on a copper grid with the use of ink formulation containing 0.88 wt % of Ag, 0.1 wt % of CMC, 1 wt % of Disperbyk-184, and 0.1 wt % of Disperbyk-181.

120 nm. This preparation of colloidal silver is the most suitable to be used as a pigment in ink-jet inks.

Ink-Jet Formulations and Printing. To achieve optimal performance, the ink-jet ink formulations should meet several requirements, such as suitable viscosity and surface tension.

Viscosity of water-based ink-jet inks in conventional office printers ranges from 1 to 8 cP. For this reason the viscosity of the silver-based ink has to be adjusted to this range. The surface tension should be adjusted to allow proper jetting from the printhead and also to allow good wetting of the substrate. For example, the

surface energy of the ink-jet transparency was found to be 42.5 mN/m, and therefore, to achieve good wetting of the transparency, the ink formulation containing silver nanoparticles should have surface tension below this value.

The viscosity of the silver dispersions was measured at 25 °C and was found to be in the range acceptable for ink-jet printing (1−3 cP at a CMC concentration in the range of 0.1−0.8 wt %). The surface tension was found to be 69.28 mN/m. Therefore, a surfactant should be added.

Evaluation of a number of formulations prepared with the use of various wetting agents, cosolvents, and surfactant were performed, and it was found that the best samples with the optimal wetting, adhesion, viscosity, and surface tension can be prepared with the use of the surfactants Disperbyk-184 (1 wt %) and Disperbyk-181 (0.1 wt %) added to dispersions containing 0.1−1.0 wt % of silver and 0.2 wt % of CMC. (We found that the addition of the surfactants did not cause a significant change in the viscosity.) It should be emphasized that the stabilizing agent, CMC, acts also as a binder to the substrate, thus providing good adhesion of ink.

Figure 11 shows a typical pattern printed with the use of the above ink formulation on an ink-jet transparency and Figure 12 presents TEM images of a single dot printed on a copper grid, at various magnifications. It appears that the dot is composed of isolated and agglomerated silver nanoparticles.

Conclusions

We presented the method for preparation of concentrated stabilized dispersions of silver nanoparticles, which can be used as pigments in ink-jet inks. CMC was found to be a very effective stabilizer for the dispersions of silver nanoparticles and also led to the formation of small particles at silver concentrations higher than previously reported. In addition, the dispersions could be further concentrated by using a lyophilization procedure, followed by redispersion of the obtained powders in a proper amount of water. Such concentrated hydrosols are characterized by the average particle size of 40−70 nm; this size increases only up to 90−120 nm after at least 7 months of storage at ambient temperature.

Silver nanoparticles obtained by redispersion of lyophilized colloids were shown to be suitable as pigments in water-based ink-jet inks. Ink formulations containing suitable surfactant and stabilizing agent, CMC, which also acts as a binder, were printed by an ink-jet printer on various substrates.

Acknowledgment. The financial support of the Israel Ministry of Industry is highly appreciated (“Magnet Program”).

CM021804B